Copper-based 2D Conductive Metal Organic Framework Thin Films for Ultrasensitive Detection of Perfluoroalkyls in Drinking Water

Aristide Gumyusenge, Tyler J. Quill, Gan Chen, Huaxin Gong, Zhenan Bao, Alberto Salleo**

Dr. A. G., T. J. Q., G. C., Dr. A. S.
Department of Materials Science and Engineering, Stanford University, Stanford, California, 94305, USA

H. G., Dr. Z. B.
Department of Chemical Engineering, Stanford University, Stanford, California, 94305, USA

E-mail: zbao@stanford.edu, asalleo@stanford.edu.

Keywords: 2D metal-organic frameworks, perfluoroalkyls, forever chemicals, bio-cumulative compounds, MOF thin-films, MOF-based sensors

Abstract

Perfluoroalkyls (PFAS) continue to emerge as a global health threat making their effective detection and capture extremely important. Though metal organic frameworks (MOF) have stood out as a promising class of porous materials for sensing PFAS, detection limits remain insufficient and fundamental understanding of detection mechanisms warrant further investigation. Here we show the use of a 2D conductive MOF film based on copper hexahydroxy triphenylene (Cu-HHTP) to fabricate a chemiresistive sensing device for detecting PFAS in drinking water. We further show ultrasensitive detection using electrochemical impedance spectroscopy. Owing to excellent electrostatic attractions and electrochemical interactions between the copper-based MOF and PFAS, the MOF-based sensor reported herein exhibits unprecedented affinity and sensitivity towards perfluorinated acids at concentrations as low as of 0.002 ng/L.

1. Introduction

Perfluoroalkyls (PFAS, also known as forever or bio-cumulative compounds) have recently emerged as a class of chemicals that urgently requires effective detection and removal.[1] These compounds, mainly perfluorooctanoic acid (PFOA) and perfluorooctanoic sulfonic acid

(PFOS), are common in industry as synthetic surfactants for the synthesis of polymer materials used in carpeting, upholstery, apparel, floor wax, textiles, firefighting foams, and sealants.[2] Despite their ubiquity, PFAS have shown to be extremely persistent in the environment. Their slow degradability has led to an overwhelming abundance in the soil, dust, air, and groundwater. Unfortunately, these compounds have also been identified as carcinogens, among many other health effects, making them a global health threat.[2] The detection and efficient removal of PFAS has thus become an important topic in recent years as these "forever chemicals" continue to be found in daily-use products and drinking water sources.[3] These environmental factors coupled with the unique physical and chemical properties of PFAS require novel materials and sensing platforms for rapid and sensitive detection of these pernicious compounds.

The typical strategy for sensitively detecting chemicals is to use high surface-area materials. In this context, metal organic frameworks (MOFs) are an attractive materials family as they provide a rich library of systems with high surface area, intrinsic porosity, and high molecular adsorptivity. They have been extensively studied for a variety of applications ranging from catalysis, energy storage, chemical capture, as well as sensing.[4–10] Particularly for MOF-based sensing, chemical tuning of metal nodes and ligands has been utilized to improve both sensitivity and selectivity towards a wide range of molecules. Identification of key functional groups out of unknown compounds have been shown and selective capturing has been achieved.[11–14] Importantly, molecular design allows MOFs to exhibit simultaneously chemical and electrical functionality. For instance, MOFs are utilized in chemiresistive devices, i.e. upon molecular uptake by the porous materials, a change in resistance is observed and utilized to identify and quantify the absorbed molecules. A few recent works have also demonstrated electrochemical sensing using MOFs as working electrodes onto which analytes can be adsorbed and detected.[7, 8] Specific to PFAS, MOFs have recently demonstrated promising affinity for the detection and removal of these chemicals. For instance, Li et al. showed that a zirconium-based MOF (NU-1000) can be used to effectively remove perfluoroalkyls from

water through adsorption of these acids onto metal sites within the framework.[16] Electrostatic attractions between PFAS and the MOF's active sites were used to rationalize the rapid and efficient adsorption compared to other porous materials.[17–20] This adsorptivity was also utilized by Cheng et al. to demonstrate ultrasensitive detection of PFOS using a mesoporous chromium-based MOF (Cr-MIL-101).[21] In that case, a MOF powder was sandwiched between two interdigitated electrodes to form a microchannel through which contaminated water was flowed. Changes in the channel resistance could be monitored to sense the presence of PFAS using impedance spectroscopy. Such devices could detect as low as 0.5 ng/L of PFOS in PBS. Despite the complicated device assembly and limited understanding on the sensing mechanism, these recent efforts show that MOFs can be used for efficient detection and capture of PFAS.

MOF-based sensors however still face major challenges mostly related to poor processability. Since these frameworks are synthesized as crystalline powders, it remains challenging to incorporate them into functional devices, which often require robust coating of active materials. In most reported device fabrication protocols, binders and additives are used to deposit MOF and immobilize particles,[11,22] which complicates the fundamental understanding of the relationship between intrinsic porosity and performance as intrinsic materials performance may be masked by extrinsic defects such as intergranular boundaries.

2D conductive MOFs (2D *c*-MOFs) have recently emerged as a type of MOF that can potentially uncover the understanding of guest-host interactions by exposing more active sites and minimizing large grain boundaries.[5,11,23–26] Such MOFs are also advantageous as they have shown to be processible into thin films.[23,27,28] Though thin film formation is still challenging and has only been demonstrated for a few MOFs, it has enabled the realization of MOF-based electronic devices. For instance, a layer-by-layer approach has been used to process copper hexahydroxyphenylene (Cu-HHTP) thin films by spray coating.[29] The 2D films showed excellent affinity towards ammonia when the MOF was coated onto interdigitated electrodes. An interfacial synthesis and film pick-up method was also recently demonstrated by Chen et al.

to form Cu-benzenehexathiol (Cu-BHT) thin films and fabricate electrochemical sensing devices.[15] This method showed to yield two types of morphologies with different densities of exposed active sites. Particularly, the bottom face with spiky metal sites showed increased sensitivity towards H_2O_2 in an electrochemical setup using the MOF film as a working electrode. Though several challenges (full understanding of molecular selectivity, sensing mechanisms, and film growth generalization) remain, these recent studies show that 2D MOF thin films are promising candidates for molecular sensing as the field evolves away from pressed pellets and powder-based devices.

Here we report a facile route to grow a 2D *c*-MOF thin film using a layer-by-layer dipping method and its use for ultrasensitive detection of most common PFAS. We show that by tuning the reaction conditions both during the film growth and during the film annealing, highly uniform, crystalline, and electrically conductive Cu-HHTP films could be produced to fabricate a sensing device in reduced processing times. We then use the 2D MOF films to sense PFOA and PFOS in water by fabricating two-terminal chemiresistive sensors. We show that by simply dipping the MOF-coated device channel into contaminated water samples, the perfluorinated acids are rapidly adsorbed onto the MOF's active sites and act as excellent oxidative agents towards the electron-rich channel. The resulting increase in the channel conductance was then used to detect traces amounts of PFAS in water. Using impedance spectroscopy measurements, we demonstrate excellent sensitivity towards the so called "forever chemicals" in water down to femtomolar concentrations.

2. Results and discussion

To fabricate MOF-based sensors, 2D copper hexahydroxy triphenylene (Cu-HHTP) MOF films were obtained through an on-surface layer-by-layer growth method (**Fig. 1**).[2830] To promote the film adhesion, we utilize a surface treatment approach to activate hydrophilic groups on the substrates. By treating our substrates with UV-Ozone exposure, effective anchoring of the metal nodes could be achieved. This labile treatment allowed us to demonstrate

a greener and simpler route (as opposed to the commonly used piranha solution treatment which is only limited to electrodes based on precious inert metals, e.g. Au,)[2830] for growing Cu-HHTP films (~10 nm per cycle) onto pre-patterned areas to fabricate desired chemiresistive sensor devices (**Fig. 1 a**). For the current study, we use commercially-available patterned ITO substrates to fabricate our sensing devices. A ligand exchange reaction could then be performed to synthesize the MOF on the substrate's surface. A continuous and uniform film was formed when the cleaned and activated substrates were alternatively immersed in solutions of copper acetate (metal source) and the hexadroxytriphenylene (ligand) as shown in **Figure 1 b**. In contrast to previous reports where the film growth takes more than 1 hour per cycle, we opted to increase the concentration of both the metal source and the ligand, and we were able to halve the growth times[28,30] After only 4 cycles (i.e. 2 hours), a continuous light-blue film could be observed by naked eye as shown in Figure S1. The film was subsequently annealed to remove any residual solvent prior to characterization and sensor fabrication.

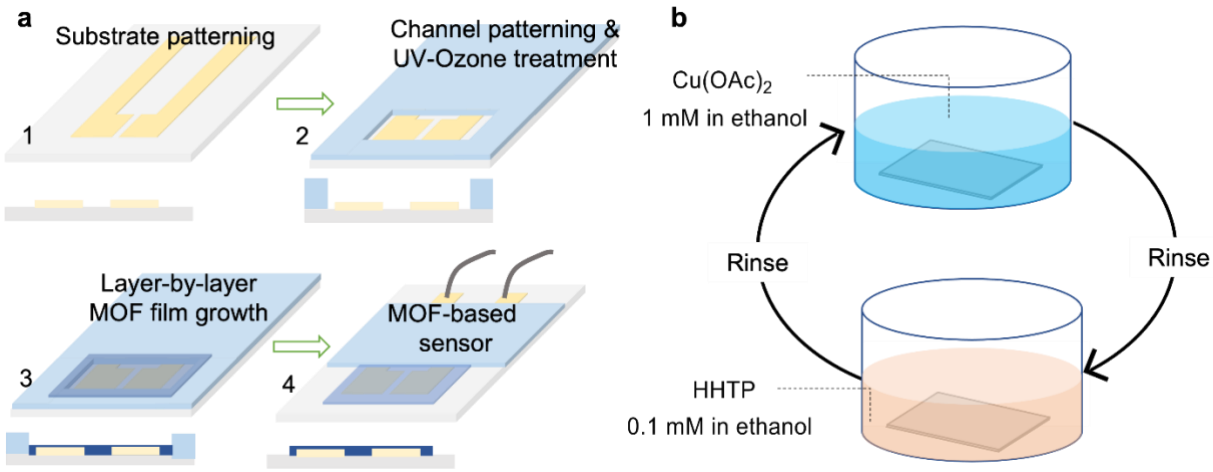

Figure 1. 2D conductive MOF film formation and sensor fabrication. **a)** Step-by-step procedure for fabricating MOF-based chemical sensing devices. **b)** Illustration of the layer-by-layer approach for the growth of Cu-HHTP films. Dilute solutions of the metal source and ligand were used for alternating anchoring and film formation.

To characterize the quality of the surface-grown MOF films, we used UV-Vis absorption spectroscopy, grazing incidence x-ray diffraction (GIXD), scanning electron microscopy (SEM), x-ray photoelectron spectroscopy (XPS), as well as energy dispersive x-

ray spectroscopy (EDX). **Figure 2 a**) shows the UV-Vis absorption spectra of Cu-HHTP annealed films revealing the characteristic light blue color of the MOF with a sharp peak around 360 nm (π–π* transition) and a broader peak around 650 nm (ligand-to-metal charge-transfer band).[30] As expected, the absorption intensity increases with the number of growth cycles, which is positively correlated with film thickness.[28,30] GIXD diffraction patterns were further used to confirm the crystallinity of the surface-grown and annealed films which has been reported before for Cu-HHTP.[30] The diffraction pattern revealed three predominant peaks both in the in-plane and out-of-plane directions as shown in **Figure 2 b**. The peaks could be indexed as the (100), (200), and (210) reflections which have previously been used to confirm the formation of the honeycomb structure of Cu-HHTP. Additionally, a broad diffraction peak around Q_z = 2.0 Å^{-1} (indexed as the 002 reflection) could be detected in both the in-plane and the out-of-plane directions (**Fig. 2 b**) suggesting that after surface anchoring, the MOF crystallites started to grow both perpendicular and parallel to the substrate. Though our grown films were not as crystalline and phase-pure as those reported when Cu-HHTP was grown on $La_{0.67}Sr_{0.33}MnO_3$ (LSMO) substrates and using longer growth times,[30] the GIXD results reveal that our method also yields crystalline and well-ordered films. SEM micrographs revealed uniformly distributed and interpenetrating MOF crystallites suggesting that the layer-by-layer method is an effective way to form continuous 2D films of Cu-HHTP (**Fig. 2 c**). This inter-penetration observed in surface-grown MOF crystallites is desired especially for MOF-based electronics where the electronic properties of pellet and powder morphologies are dominated by the grain boundaries.[31]

XPS elemental analysis was further used to confirm the MOF structure from the predicted coordination. Characteristic binding energies were measured and confirmed as shown in **Figure 2 d** and Fig. S2. All expected elements and corresponding binding energies could be detected in the 2D films. Most importantly, a strong Cu^{2+} peak was observed around 935 eV with a shoulder peak around 933 eV assigned to Cu^{1+} accompanied by a strong satellite peak

around 943 eV. These peak positions and ratios support the MO_4 coordination and the bivalent nature of the metal for charge balance.[24,25,32] The bivalent nature of the metal atoms has been previously used to support the semiquinonate and catecholate states for HHTP ligands especially in Cu-based MOFs; the metal exists in its +1 and +2 states to form a neutral structure.[32,33] Furthermore, compositional uniformity could be confirmed in our surface-grown MOF films by the mappings generated from SEM-EDX mapping (**Fig. 2 c-e**, and Fig. S3). Both the copper signal and elemental composition from the ligand remain uniform across the grown film showing effective reactivity on the substrate's surface to form a homogeneous Cu-HHTP thin film. This uniform distribution of metal active sites was desired for efficient exposure and adsorption of target analytes especially for sensing applications. Film uniformity in combination with reduced growth times is key towards the realization of 2D MOF-based electronics where continuous and highly conductive films are desirable yet challenging to process.

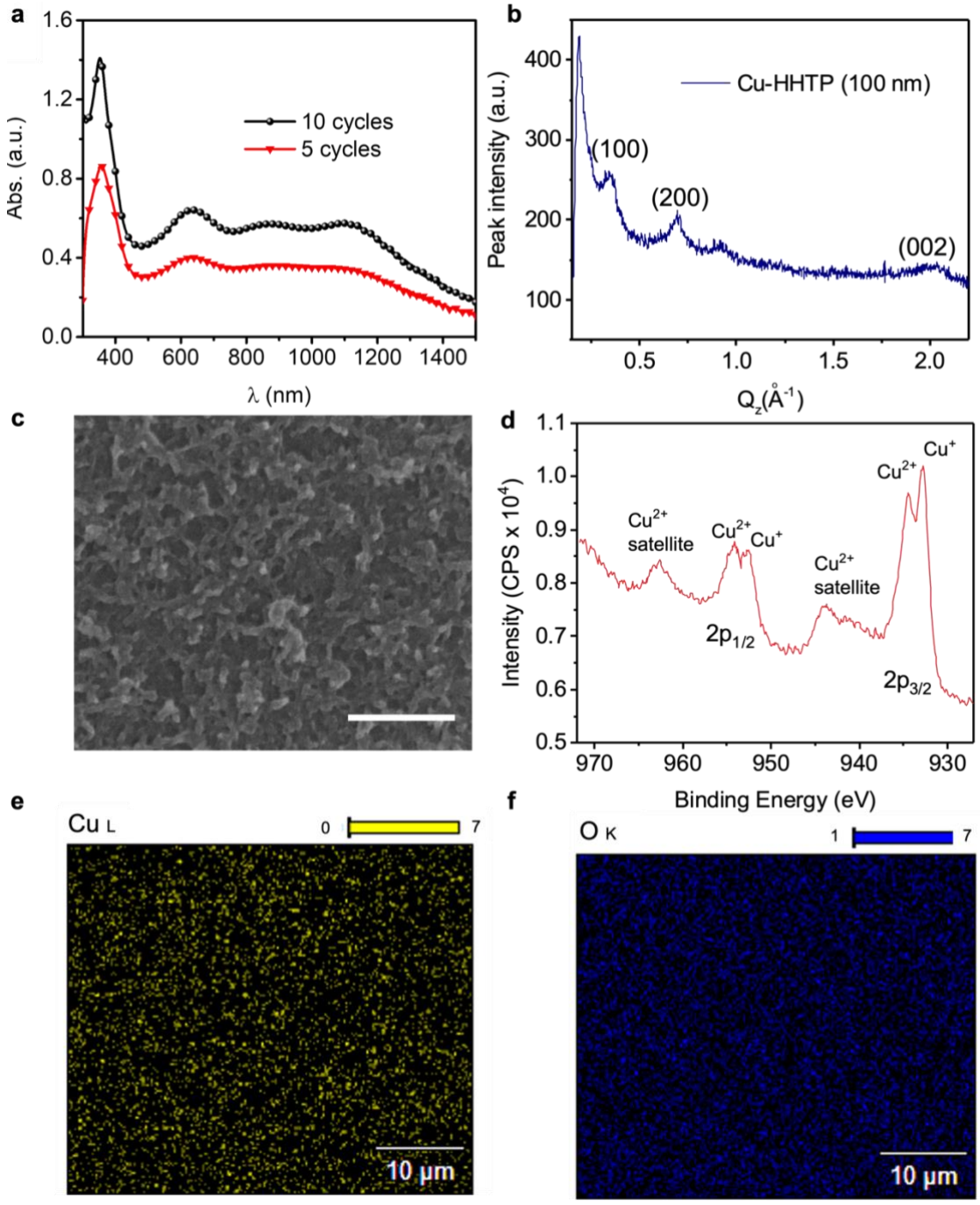

Figure 2. Cu-HHTP MOF film characterization. **a)** Thickness dependent UV-Vis absorption. **b)** Out-of-plane x-ray diffraction pattern from a Cu-HHTP film. **c)** SEM image of the 2D film on ITO showing interconnected crystallites of MOF formed on the surface. The scale bar represents 200 nm. **d)** High resolution XPS spectra of the signature copper peaks. A strong Cu^{2+} peak is observed along with corresponding satellite peak. A Cu^{1+} could also be detected a lower binding energies. **e), f)** Elemental mapping generated by EDX spectra showing a highly uniform distribution of all elements.

After confirming the formation of the Cu-HHTP MOF into thin films, we probed the functionality of the material towards molecular sensing especially targeting water contaminants. It has been shown that in quaternary-coordinated MOFs, the MO_4 sites tend to

exhibit a residual negative charge as shown in **Figure 3 a**.[24,32,33] Furthermore, the predominant charged species is expected to readily undergo oxidative reactions without disturbing the corresponding coordination owing to the bivalent nature of the metal atoms.[34] With abundant electron-rich sites exposed in our 2D films, we envision that Cu-HHTP would be ideal for sensing electron-deficient species. In addition, the oxygen-rich coordination sites render the Cu-HHTP MOF film predominantly hydrophilic, making it an ideal candidate towards analytes with hydrophilic ends.

We thus targeted the sensing of perfluoroalkyls (PFAS) which are comprised of a hydrophilic head with an acidic hydrogen (either carboxylic or sulfonic) and a fluorine-rich hydrophobic tail.[35] We expect such amphiphilic nature to enable strong electrostatic interactions between our Cu-HHTP films and PFAS owing to both i) the residual negative charge along the coordination sites and, ii) the hydrophilic nature of the MOF from the oxygen-rich ligand. In addition, the unique chemical structure of PFAS distinguishes them from other common water contaminants (e.g. inorganic salts) allowing the selectivity towards these larger and highly polar analytes easier to engineer. We thus tested the sensitivity of our Cu-HHTP films towards PFAS with the rationale that the electronic cloud present at each coordination nodes within the MOF would lead to strong electrostatic attractions between the MOF films and PFAS. Upon adsorption of a PFA, we expect electrostatic interactions between our electron-rich MOF and the fluorinated tail to alter the overall oxidation of Cu-HHTP. The change in film conductivity would be used for detection. This sensing mechanism was also inspired by the recent success of MOFs (e.g. NU-1000, Cr-MIL-101) towards adsorbing PFAS in water.[16,18,21,36] We aimed to enhance such adsorptive sensitivity by exposing more active metal sites on the surface of our MOF films, as opposed to the previously reported adsorb-to-capture approach in powder-based platforms.[16,18,21,36] Since we expect that other oxidative pollutants might have a similar effect on the MOF, thus making selectivity a challenging task especially in ground water samples, we targeted to test the presence of PFAS in drinking water for proof of concept. Here, common

pollutants (e.g. salts) have been well studied and can be filtered out using ubiquitous methods, but PFAS, in addition to requiring more sophisticated and costly treatment techniques (e.g. powdered activated carbon and nanofiltration), remain difficult to remove owing to their physicochemical properties, thus posing a major threat when undetected.[37] We chose to sense the two most common PFAS: perfluorooctanoic acid (PFOA) and its sulfonic acid analogue (PFOS) and tested their adsorption onto Cu-HHTP in water samples.

The oxidation of Cu-HHTP was indeed observed when the MOF thin film on ITO electrodes was dipped into a sample of water contaminated by different amounts of PFOA. The current-voltage (*I-V*) curves in **Figure 3 b** show an increase in film conductivity with increasing amount of PFOA added into the water. This increase in the current response from a two-terminal device was a first, simple, and yet clear indicator that Cu-HHTP becomes oxidized in the presence of aqueous PFAS. Cyclic voltammograms obtained with Cu-HHTP films as a working electrode (versus an Ag/AgCl reference and a Pt mesh as the counter electrode) in PBS also showed an obvious increase in the MOF's oxidation and reduction activity when pristine PBS was compared to a 10 nM PFOA solution in PBS (**Fig. 3 c**). A strong and reversible oxidation peak around 0.312 V (with a reduction peak detected at -0.315 V) emerged when PFOA was added into the electrolyte. A control experiment in which the same potential was applied to the electrochemical cell, but in the absence of Cu-HHTP onto the ITO-working electrode, i.e. a bare ITO working as the working electrode, showed no redox activity from PFOA alone (Fig. S4). This electrochemical behavior suggests that the observed redox activity within the scanned potential window results from the interactions between the Cu-HHTP MOF film and the PFA. Though oxygen reduction side reactions are anticipated in our testing conditions contributing overall charge neutrality in solution,[38,39] Cu-HHTP is able to maintain a stable oxidized structure as shown in **Figure 3 a** upon adsorption of the PFAS.

To probe this oxidative interaction of Cu-HHTP and fluorinated compounds at a molecular level, we carried out systematic elemental analysis using XPS and compared the

pristine Cu-HHTP films to those exposed to PFAS. XPS spectra of Cu-HTTP films before and after exposure to PFOA solutions revealed substantial changes in oxidation states on the MOF's coordination center as shown in **Figure 3 d, e** and Fig. S5. Noticeably, after exposure, the relative ratio of Cu^{1+} to Cu^{+2} in the MOF decreased, indicating that the presence of PFAS results in substantial changes in the oxidation state of the copper atoms, which as stated above, are key species towards maintaining charge neutrality within the MOF.[24,32,33,40,41] The observed changes in oxidation state of copper should be accompanied by changes in binding energy of the oxygen atoms along the periphery of the copper center, which is what we observe after exposing Cu-HHTP to PFOA. Indeed, the location of maximum intensity in the O 1s XPS spectra shifts to higher binding energy, accompanied by a change in peak shape as Cu-HTTP switches between its benzenoid and quinoid forms (**Fig. 3 d, e**).[5,32,33] A similar behavior is also observed when PFOS is used as the analyte (Fig. S5) suggesting that in presence of PFAS, the MOF adopts its quinoid form to balance the electronic charge along its coordination sites.

We also confirmed the adsorption of the PFA into the bulk of the MOF film using XPS as shown in Fig. S6. We carried out XPS measurements on Cu-HHTP films after casting a 10 nM PFOA solution and measuring the binding energies of F atoms. We found that at the surface, unbound or "free" F atoms exhibit a negligible difference (< 1 eV) in binding energy from the atoms probed after sputtering deep into the MOF film analogous to previous reports.[21] Note that higher peak intensities were found at the surface as the majority of PFOA most likely remains on the surface upon drying. This sensitivity of the Cu-HHTP films towards the fluorinated analytes could also be visualized with the naked eye when a drop of the stock PFOS solution was dropped on a MOF-coated glass. The coloration of the MOF film showed to bleach immediately after PFOS was cast onto it (Fig S7). Such change in MOF film coloration has also been shown when doping MOFs with electron-acceptors such as 2,3,5,6-Tetrafluoro-7,7,8,8-tetracyanoquinodimethane (F4-TCNQ).[31] We expect that the color change, and the concomitant increase in film conductivity, is due to the oxidation of Cu-HHTP by the electron-

deficient analytes that can abduct electrons from the MOF's active sites as evidenced by our electrochemistry results.

The observed oxidation of the MOF film also showed to be non-destructive for the MOF structure. Despite the coloration change most likely due to the overall change in charge along the active site, the structure of the MOF remained intact after dipping in PFAS and washing. The elemental composition of the MOF film was found to remain unchanged as evidenced from the post-sensing XPS spectra (Fig. S8). This structural stability towards the oxidative adsorption of PFAS in Cu-HHTP as well as the efficient release of sensed PFA molecules was rationalized by the fact that the key interactions between the MOF and the analyte are due to surface electrostatics that are electronically detectable yet reversible especially at low PFA concentrations. This behavior is enabled by the thin film platform we utilize as opposed to previously studied powders (oftentimes using morphological binders) that rely on the binding and trapping of the analyte.[21,29] In our film-based devices, we expect a high density of the metal active sites on the surface, which would translate to a highly sensitive bind-and-release mechanism even at low analyte concentrations.

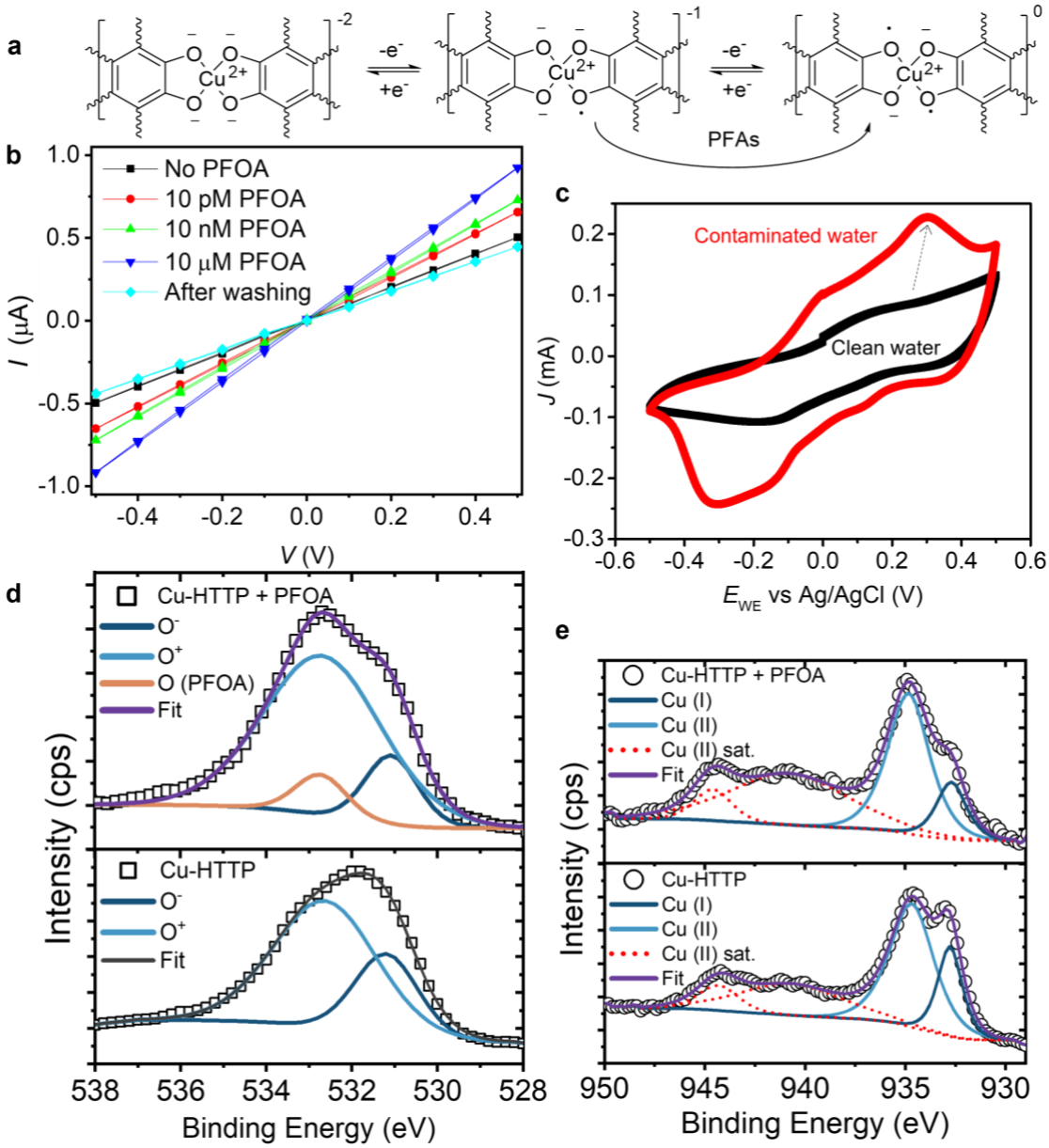

Figure 3. MOF affinity towards PFAS. **a)** Schematic illustration of the charge distribution across the MOF's active sites. An overall negative charge at each coordination node is expected. **b)** *I-V* curves from a MOF film dipped in water with different levels of PFOA contamination. The film conductance shows to nearly double upon contact with the fluorinated acid. **c)** Increase in red-ox activity of Cu-HHTP film when pristine PBS is compared to contaminated (10 nM PFOA) PBS. **d), e)** High resolution XPS spectra of the O and Cu peaks, respectively, comparing intensity changes before (bottom) and after (top) exposure of Cu-HHTP to PFOA. The two binding energy peaks for oxygen are labelled as O^- and O^+ for clarity.

We then tested the sensitivity of our MOF films towards PFAS using electrochemical impedance spectroscopy (EIS) as a means to monitor the change in channel conductance, where spurious effects, such as resistance to current injection, don't affect sensitivity. The simple device architecture of our studied MOF-based sensor is shown in **Figure 4 a**. We employ a 2-

terminal device layout which has been previously shown to be effective for recording EIS changes in resistance-dominated systems.[21,42–44] More specifically, we record the changes in the device impedance at high frequencies (1kHz – 1MHz). The device could be used either by dropping an aqueous sample onto the channel or by fully immersing the MOF-covered channel into contaminated water. We carried out the sensing in a PBS 0.1x standard by immersing the MOF channel with various contamination levels (i.e., PFA concentration). **Figure 4 c**, **d**, and Fig. S 9-10 show EIS spectra from representative devices when immersed in PBS with increasing amounts of PFOA. The device resistance showed to decrease significantly upon immersion, even when as little as 10 fM of the fluorinated acid was present. With careful dilution of the analyte solution, we found a detection limit of our MOF-based sensor to be as low as 5 fM (or 0.002 ng/L of PFOA) as shown in **Figure 4 d & e**. Such sensitivity could be attributed to the high surface area of our MOF films, as well as the chemical affinity of the metal active sites towards the fluorinated acid. Furthermore, we tested 10 different devices and showed a linear correlation ($R^2 > 0.968$) between the conductance and the logarithm of PFAS concentration (**Fig. 4 e**) indicative of the reliability of the MOF film approach. A similar behavior was also observed when the MOF-based sensor was used to detect PFOS, another common PFA (**Fig. 4 f**). As previously mentioned, the PFA sensing is based on the adsorption of the PFAS molecules onto the MOFs sites which further allowed our sensors to be used at least 10 times without declining performance (Fig. S11). Here we tested the reusability of the sensing device at low (10 nM) PFAS concentration and showed that the device exhibits reversible resistance change even after 10 cycles, likely due to abundant binding sites at the film interface. This excellent sensitivity towards PFAS in MOF-based devices contrasted with a control device where a bare channel used and immersed in contaminated water similarly to the MOF-based sensor. The bare channel shows an increase in resistance when PFOA was introduced in PBS (Fig. S12) as expected after introducing non-conductive analytes. Given the sensitivity of impedance spectroscopy towards electrolyte compositional changes, the observed

decrease in our MOF film resistance while the electrolyte resistance increases proves that the material is indeed sensing the analyte. Such working mechanism using Cu-HHTP allows us to efficiently detect oxidative agents (in this case PFAS) especially in water using a robust and affordable setup.

The MOF-based sensors we demonstrate are easy to fabricate, scalable, and offer readouts in minutes as opposed to other techniques such as mass spectrometry (liquid chromatography tandem mass spectrometry, time-of-flight mass spectrometry) which involve long sample preparation and data acquisition times.[45,46] In fact, our sensors show to be extremely sensitive (with a detection limit as low as 0.002 ng/L) towards the two most common PFAS (PFOA and PFOS) proving to detect these compounds well below their health advisory levels (HALs) recommended by the US environmental protection agency (EPA) and the food and drug administration (FDA). In drinking water, the HALs for these two acids have been set to as low as 10 ng/L.[21] The MOF-based sensor could detect both PFOA and PFOS at concentrations nearly 4 orders of magnitude below these suggested levels (**Fig. 4 e**), and more than 2 orders of magnitude better than the best reported sensitivity levels by sensors using MOF adsorption as the sensing mechanism.[21] With the sensitivity levels achieved herein, our thin film approach shows to be a viable and reliable platform towards sensing PFAS even in samples where large amounts are yet to accumulate. Though the proposed sensing platform based on the oxidation of the MOF layer upon PFAS adsorption warrants further systematic investigation on whether different PFAS can be selectively identified, the ultrasensitive detection we demonstrated is a great complement to current efforts on tracing and capturing these highly resilient compounds that continue to pose a global health threat.

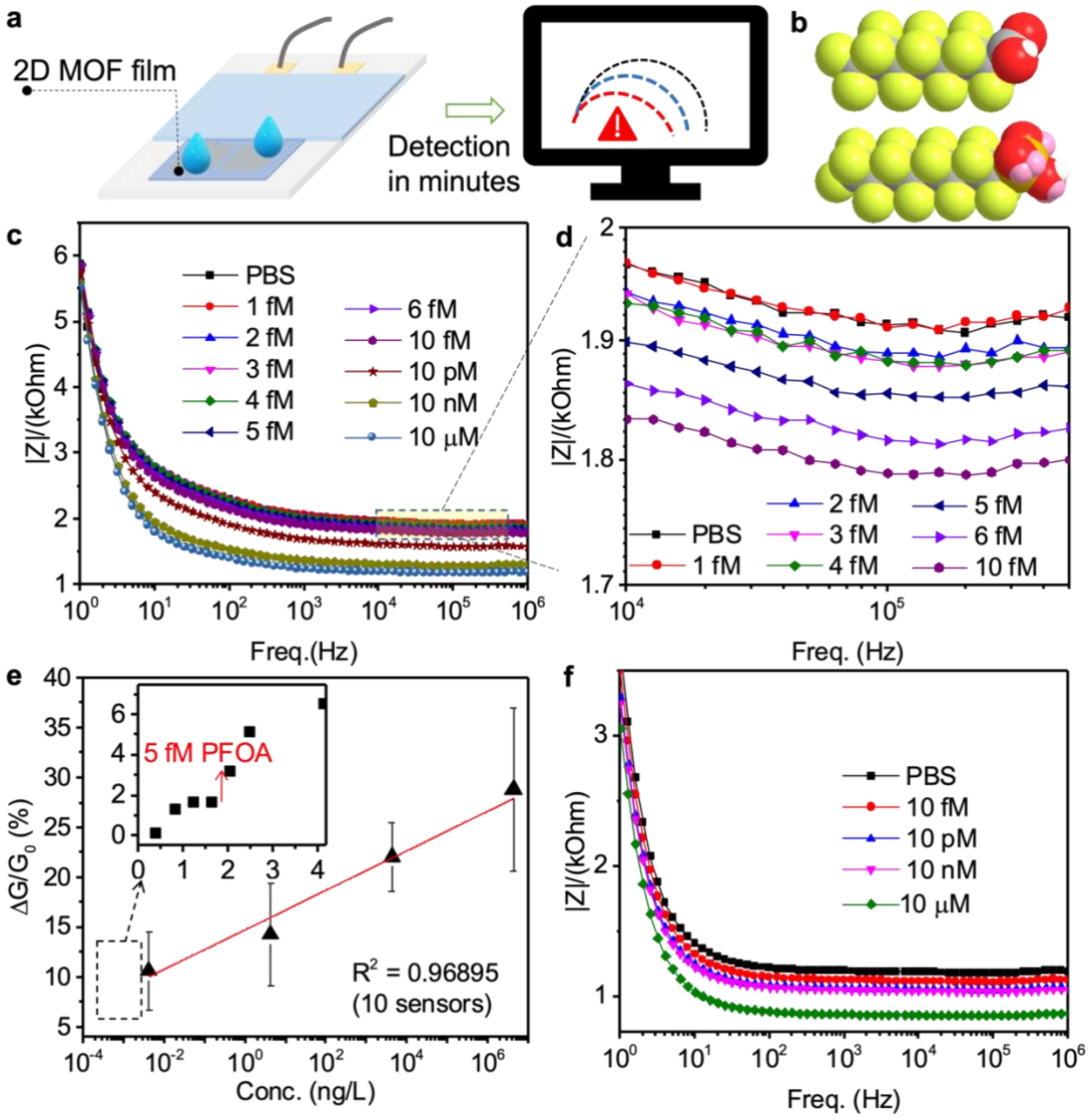

Figure 4. Ultrasensitive detection of PFAS using a 2D MOF-based sensor. **a)** Illustration of MOF-based sensor. The MOF-coated channel is used to adsorb PFAS in water samples and the changes in channel resistance are recorded using impedance spectroscopy. **b)** Chemical structure of PFOA and PFOS showing the hydrophilic heads and hydrophobic (fluorine-rich) tails. **c), d) e)** Correlation between the device channel conductance change and the concentration of PFOA in PBS. The Bode plots were obtained from a representative device at very low PFOA concentrations, and calibration curve was obtained from 10 different representative sensors. Cu-HHTP films showed to detect PFOA at concentrations as low as 5 fM in PBS. An R^2 value of 0.968 could be achieved from 10 different devices. **f)** Bode plots recorded from the MOF channel when different amounts of PFOS are added into PBS solution.

3. Conclusions

We demonstrated a simple device design for detecting perfluoroalkyls using 2D MOF thin films. Uniform films of Cu-HHTP could be readily processed through a layer-by-layer growth method. This facile film formation procedure allowed to fabricate two-terminal resistive

sensor with unprecedented sensitivity towards PFOA and PFOS, the most common PFAS. We carried out full characterization of the formed films to showcase that the 2D nature of our films are key to exposing more active sites and thus attaining high sensitivity towards the analytes of interest. We show that the electron-rich MOF sites are advantageous for detecting the amphiphilic bio-cumulative chemicals in water.

Experimental Section

Materials: Copper acetate, phosphate-buffered saline (PBS 10x), pure ethyl alcohol, perfluorooctanoic acid (PFOA) and perfluorooctanesulfonic acid (PFOS) (40% in water) were purchased from Sigma Aldrich and used as received. Hexahydroxy triphenylene (HHTP) was purchased from ACROS Organics. Copper acetate and HHTP were first dissolved in ethanol (1 mM and 0.1 mM, respectively) and allowed to stir for at least 30 mins at ambient. Phosphate-buffered saline (10x) was used to obtain 0.1x after dilution using distilled water. PFOA was first dissolved in distilled water and allowed to stir overnight before use. PFOS stock solution was used as received. Different concentrations of PFAS were obtained by diluting dissolved PFOA and stock PFOS in PBS.

Substrate treatment: Glass substrates with ITO-stripes were first sonicated in water, acetone, and isopropanol successively for 5 mins then dried with pure N_2. The cleaned substrates were then treated under UV-ozone lamp for 30 mins. This contrasted with harsher (piranha treatment)[30] alternative which tends to etch away the ITO. Using the more benign surface treatment allowed to pre-determine the film growth area by covering the undesired areas with acrylic tape. The ozone treated substrates were then immediately immersed into the salt solution for film growth.

MOF film growth: A 1 mM solution of copper acetate was first pulled over treated substrates and allowed adhere onto the surface for 10 mins. The substrates were then carefully rinsed by dipping in fresh ethanol before being transferred into another container with a 0.1 mM solution of HHTP ligand in ethanol. The ligand exchange on the substrate surface was then allowed to proceed for 20 minutes without disturbance at ambient. After rinsing off unreacted ligands with fresh ethanol, the dipping steps were repeated to desired film thickness. The films were then annealed at 80 °C inside a N_2-filled glovebox prior to characterization.

Morphology analysis: The UV-Vis absorption spectra were collected using an Agilent Cary 6000i UV/Vis/NIR on MOF films grown on cleaned glass substrates. SEM images were taken using a FEI Magellan 400 XHR Scanning Electron Microscope (SEM) with FEG source on films grown either on ITO coated glass or Si substrates.

Elemental analysis: XPS measurements were performed using PHI Versa Probe 3 XPS with a monochromatized Al source (1486.6 eV; 50 W; 200 µm spot size). An electron flood gun and low energy Ar^+ ions were used to neutralize the sample and prevent charging. Binding energies were calibrated to the adventitious carbon peak at 284.8 eV and smoothed using a 5-point quadradic Savitzki-Golay method in CasaXPS software. Scans were taken with a pass energy of 55 eV or 112 eV. Depth profiles were performed by sputtered with a gas cluster ion source (10 kV Ar^+_{2500}) to minimize sample damage and preserve relevant chemistry.

GIXD: X-ray diffraction measurements were performed at the Stanford Synchrotron Radiation Lightsource (SSRL) on beam line 11-3 using an area detector and incident energy 12.73 keV. The sample to detector distance was 317.06 mm and was calibrated using a polycrystalline LaB6 standard. The incidence angle used in all measurements was 0.1° slightly larger than the critical angle and measurements were performed in a helium chamber to minimize scattering

from air. All data was corrected for the geometric distortion of the flat detector used analyzed using Nika 1D SAXS[47] and WAXstools[48] software in Igor Pro.

Electrical characterization: *I-V* curves were collected using a Keithley 2612 Source Meter LabVIEW as a software. Electrochemical impedance spectroscopy was performed on a Bio-Logic SP-300 using a sinusoidal AC amplitude of 10 mV over a frequency range of 1 Hz –1 MHz. Cyclic voltammetry measurements were carried out using a Bio-Logic SP-300 with a leakless Ag/AgCl reference electrode, a Pt mesh as the counter electrode, and 20 mV/s as the scan rate.

Acknowledgements

A.G. and A. S acknowledge the financial support from the Geballe Laboratory for Advanced Materials (GLAM) Fellowship. T.J.Q. gratefully acknowledges support from the NSF Graduate Research Fellowship Program under grant DGE-1656518. Part of this work was performed at the Stanford Nano Shared Facilities (SNSF), supported by the National Science Foundation under award ECCS-2026822 and the Stanford Synchrotron Radiation Lightsource, SLAC National Accelerator Laboratory, which is supported by the U.S. Department of Energy, Office of Science, Office of Basic Energy Sciences under Contract No. DE-AC02-76SF00515.

References

(1) Peer Reviewed: Perfluorochemical Surfactants in the Environment. *Environ. Sci. Technol.* **2002**, *36* (7), 146A-152A. https://doi.org/10.1021/es022253t.

(2) Nicole, W. PFOA and Cancer in a Highly Exposed Community: New Findings from the C8 Science Panel. *Environ. Health Perspect.* **2013**, *121* (11–12), A340–A340. https://doi.org/10.1289/ehp.121-A340.

(3) Hu, X. C.; Andrews, D. Q.; Lindstrom, A. B.; Bruton, T. A.; Schaider, L. A.; Grandjean, P.; Lohmann, R.; Carignan, C. C.; Blum, A.; Balan, S. A.; Higgins, C. P.; Sunderland, E. M. Detection of Poly- and Perfluoroalkyl Substances (PFASs) in U.S. Drinking Water Linked to Industrial Sites, Military Fire Training Areas, and Wastewater Treatment Plants. *Environ. Sci. Technol. Lett.* **2016**, *3* (10), 344–350. https://doi.org/10.1021/ACS.ESTLETT.6B00260/SUPPL_FILE/EZ6B00260_SI_001.PDF.

(4) Lee, J.; Farha, O. K.; Roberts, J.; Scheidt, K. A.; Nguyen, S. T.; Hupp, J. T. Metal–Organic Framework Materials as Catalysts. *Chem. Soc. Rev.* **2009**, *38* (5), 1450–1459. https://doi.org/10.1039/B807080F.

(5) Nam, K. W.; Park, S. S.; dos Reis, R.; Dravid, V. P.; Kim, H.; Mirkin, C. A.; Stoddart, J. F. Conductive 2D Metal-Organic Framework for High-Performance Cathodes in Aqueous Rechargeable Zinc Batteries. *Nat. Commun.* **2019**, *10* (1), 4948. https://doi.org/10.1038/s41467-019-12857-4.

(6) Liu, W.; Yin, X.-B. Metal–Organic Frameworks for Electrochemical Applications. *TrAC Trends Anal. Chem.* **2016**, *75*, 86–96. https://doi.org/https://doi.org/10.1016/j.trac.2015.07.011.
(7) Liu, J.; Chen, Z.; Wang, R.; Alayoglu, S.; Islamoglu, T.; Lee, S.-J.; Sheridan, T. R.; Chen, H.; Snurr, R. Q.; Farha, O. K.; Hupp, J. T. Zirconium Metal–Organic Frameworks Integrating Chloride Ions for Ammonia Capture and/or Chemical Separation. *ACS Appl. Mater. Interfaces* **2021**, *13* (19), 22485–22494. https://doi.org/10.1021/acsami.1c03717.
(8) Allendorf, M. D.; Dong, R.; Feng, X.; Kaskel, S.; Matoga, D.; Stavila, V. Electronic Devices Using Open Framework Materials. *Chem. Rev.* **2020**, *120* (16), 8581–8640. https://doi.org/10.1021/acs.chemrev.0c00033.
(9) Hexiang, D.; Sergio, G.; E., C. K.; Cory, V.; Hiroyasu, F.; Mohamad, H.; Felipe, G.; C., W. A.; Zheng, L.; Shunsuke, A.; Hiroyoshi, K.; Michael, O.; Osamu, T.; Fraser, S. J.; M., Y. O. Large-Pore Apertures in a Series of Metal-Organic Frameworks. *Science* **2012**, *336* (6084), 1018–1023. https://doi.org/10.1126/science.1220131.
(10) Farha, O. K.; Eryazici, I.; Jeong, N. C.; Hauser, B. G.; Wilmer, C. E.; Sarjeant, A. A.; Snurr, R. Q.; Nguyen, S. T.; Yazaydın, A. Ö.; Hupp, J. T. Metal–Organic Framework Materials with Ultrahigh Surface Areas: Is the Sky the Limit? *J. Am. Chem. Soc.* **2012**, *134* (36), 15016–15021. https://doi.org/10.1021/ja3055639.
(11) Campbell, M. G.; Liu, S. F.; Swager, T. M.; Dincă, M. Chemiresistive Sensor Arrays from Conductive 2D Metal–Organic Frameworks. *J. Am. Chem. Soc.* **2015**, *137* (43), 13780–13783. https://doi.org/10.1021/jacs.5b09600.
(12) Assen, A. H.; Yassine, O.; Shekhah, O.; Eddaoudi, M.; Salama, K. N. MOFs for the Sensitive Detection of Ammonia: Deployment of Fcu-MOF Thin Films as Effective Chemical Capacitive Sensors. *ACS Sensors* **2017**, *2* (9), 1294–1301. https://doi.org/10.1021/acssensors.7b00304.
(13) Campbell, M. G.; Sheberla, D.; Liu, S. F.; Swager, T. M.; Dincă, M. Cu3(Hexaiminotriphenylene)2: An Electrically Conductive 2D Metal–Organic Framework for Chemiresistive Sensing. *Angew. Chemie Int. Ed.* **2015**, *54* (14), 4349–4352. https://doi.org/https://doi.org/10.1002/anie.201411854.
(14) Lyu, P.; Wright, A. M.; López-Olvera, A.; Mileo, P. G. M.; Zárate, J. A.; Martínez-Ahumada, E.; Martis, V.; Williams, D. R.; Dincă, M.; Ibarra, I. A.; Maurin, G. Ammonia Capture via an Unconventional Reversible Guest-Induced Metal-Linker Bond Dynamics in a Highly Stable Metal–Organic Framework. *Chem. Mater.* **2021**, *33* (15), 6186–6192. https://doi.org/10.1021/acs.chemmater.1c01838.
(15) Chen, X.; Dong, J.; Chi, K.; Wang, L.; Xiao, F.; Wang, S.; Zhao, Y.; Liu, Y. Electrically Conductive Metal–Organic Framework Thin Film-Based On-Chip Micro-Biosensor: A Platform to Unravel Surface Morphology-Dependent Biosensing. *Adv. Funct. Mater.* **2021**, *n/a* (n/a), 2102855. https://doi.org/https://doi.org/10.1002/adfm.202102855.
(16) Li, R.; Alomari, S.; Stanton, R.; Wasson, M. C.; Islamoglu, T.; Farha, O. K.; Holsen, T. M.; Thagard, S. M.; Trivedi, D. J.; Wriedt, M. Efficient Removal of Per- and Polyfluoroalkyl Substances from Water with Zirconium-Based Metal–Organic Frameworks. *Chem. Mater.* **2021**, *33* (9), 3276–3285. https://doi.org/10.1021/acs.chemmater.1c00324.
(17) Clark, C. A.; Heck, K. N.; Powell, C. D.; Wong, M. S. Highly Defective UiO-66 Materials for the Adsorptive Removal of Perfluorooctanesulfonate. *ACS Sustain. Chem. Eng.* **2019**, *7* (7), 6619–6628. https://doi.org/10.1021/acssuschemeng.8b05572.
(18) Liu, K.; Zhang, S.; Hu, X.; Zhang, K.; Roy, A.; Yu, G. Understanding the Adsorption of PFOA on MIL-101(Cr)-Based Anionic-Exchange Metal–Organic Frameworks: Comparing DFT Calculations with Aqueous Sorption Experiments. *Environ. Sci.*

Technol. **2015**, *49* (14), 8657–8665. https://doi.org/10.1021/acs.est.5b00802.
(19) Barpaga, D.; Zheng, J.; Han, K. S.; Soltis, J. A.; Shutthanandan, V.; Basuray, S.; McGrail, B. P.; Chatterjee, S.; Motkuri, R. K. Probing the Sorption of Perfluorooctanesulfonate Using Mesoporous Metal–Organic Frameworks from Aqueous Solutions. *Inorg. Chem.* **2019**, *58* (13), 8339–8346. https://doi.org/10.1021/acs.inorgchem.9b00380.
(20) Chen, B.; Yang, Z.; Qu, X.; Zheng, S.; Yin, D.; Fu, H. Screening and Discrimination of Perfluoroalkyl Substances in Aqueous Solution Using a Luminescent Metal–Organic Framework Sensor Array. *ACS Appl. Mater. Interfaces* **2021**. https://doi.org/10.1021/acsami.1c15528.
(21) Cheng, Y. H.; Barpaga, D.; Soltis, J. A.; Shutthanandan, V.; Kargupta, R.; Han, K. S.; McGrail, B. P.; Motkuri, R. K.; Basuray, S.; Chatterjee, S. Metal–Organic Framework-Based Microfluidic Impedance Sensor Platform for Ultrasensitive Detection of Perfluorooctanesulfonate. *ACS Appl. Mater. Interfaces* **2020**, *12* (9), 10503–10514. https://doi.org/10.1021/acsami.9b22445.
(22) Feng, D.; Lei, T.; Lukatskaya, M. R.; Park, J.; Huang, Z.; Lee, M.; Shaw, L.; Chen, S.; Yakovenko, A. A.; Kulkarni, A.; Xiao, J.; Fredrickson, K.; Tok, J. B.; Zou, X.; Cui, Y.; Bao, Z. Robust and Conductive Two-Dimensional Metal−organic Frameworks with Exceptionally High Volumetric and Areal Capacitance. *Nat. Energy* **2018**, *3* (1), 30–36. https://doi.org/10.1038/s41560-017-0044-5.
(23) Cui, Y.; Yan, J.; Chen, Z.; Zhang, J.; Zou, Y.; Sun, Y.; Xu, W.; Zhu, D. [Cu3(C6Se6)]n: The First Highly Conductive 2D π–d Conjugated Coordination Polymer Based on Benzenehexaselenolate. *Adv. Sci.* **2019**, *6* (9), 1802235. https://doi.org/https://doi.org/10.1002/advs.201802235.
(24) Park, J.; Hinckley, A. C.; Huang, Z.; Feng, D.; Yakovenko, A. A.; Lee, M.; Chen, S.; Zou, X.; Bao, Z. Synthetic Routes for a 2D Semiconductive Copper Hexahydroxybenzene Metal–Organic Framework. *J. Am. Chem. Soc.* **2018**, *140* (44), 14533–14537. https://doi.org/10.1021/jacs.8b06666.
(25) Dou, J.-H.; Arguilla, M. Q.; Luo, Y.; Li, J.; Zhang, W.; Sun, L.; Mancuso, J. L.; Yang, L.; Chen, T.; Parent, L. R.; Skorupskii, G.; Libretto, N. J.; Sun, C.; Yang, M. C.; Dip, P. V.; Brignole, E. J.; Miller, J. T.; Kong, J.; Hendon, C. H.; Sun, J.; Dincă, M. Atomically Precise Single-Crystal Structures of Electrically Conducting 2D Metal–Organic Frameworks. *Nat. Mater.* **2021**, *20* (2), 222–228. https://doi.org/10.1038/s41563-020-00847-7.
(26) Park, J.; Lee, M.; Feng, D.; Huang, Z.; Hinckley, A. C.; Yakovenko, A.; Zou, X.; Cui, Y.; Bao, Z. Stabilization of Hexaaminobenzene in a 2D Conductive Metal–Organic Framework for High Power Sodium Storage. *J. Am. Chem. Soc.* **2018**, *140* (32), 10315–10323. https://doi.org/10.1021/jacs.8b06020.
(27) Miao, Y.; Tsapatsis, M. Electron Beam Patterning of Metal–Organic Frameworks. *Chem. Mater.* **2021**, *33* (2), 754–760. https://doi.org/10.1021/acs.chemmater.0c04204.
(28) Liu, Y.; Wei, Y.; Liu, M.; Bai, Y.; Wang, X.; Shang, S.; Du, C.; Gao, W.; Chen, J.; Liu, Y. Face-to-Face Growth of Wafer-Scale 2D Semiconducting MOF Films on Dielectric Substrates. *Adv. Mater.* **2021**, *33* (13), 2007741. https://doi.org/https://doi.org/10.1002/adma.202007741.
(29) Yao, M.-S.; Lv, X.-J.; Fu, Z.-H.; Li, W.-H.; Deng, W.-H.; Wu, G.-D.; Xu, G. Layer-by-Layer Assembled Conductive Metal–Organic Framework Nanofilms for Room-Temperature Chemiresistive Sensing. *Angew. Chemie Int. Ed.* **2017**, *56* (52), 16510–16514. https://doi.org/https://doi.org/10.1002/anie.201709558.
(30) Song, X.; Wang, X.; Li, Y.; Zheng, C.; Zhang, B.; Di, C.; Li, F.; Jin, C.; Mi, W.; Chen, L.; Hu, W. 2D Semiconducting Metal–Organic Framework Thin Films for Organic Spin Valves. *Angew. Chemie Int. Ed.* **2020**, *59* (3), 1118–1123.

https://doi.org/https://doi.org/10.1002/anie.201911543.
(31) Stavila, V.; Talin, A. A.; Allendorf, M. D. MOF-Based Electronic and Opto-Electronic Devices. *Chem. Soc. Rev.* **2014**, *43* (16), 5994–6010. https://doi.org/10.1039/C4CS00096J.
(32) Darago, L. E.; Aubrey, M. L.; Yu, C. J.; Gonzalez, M. I.; Long, J. R. Electronic Conductivity, Ferrimagnetic Ordering, and Reductive Insertion Mediated by Organic Mixed-Valence in a Ferric Semiquinoid Metal–Organic Framework. *J. Am. Chem. Soc.* **2015**, *137* (50), 15703–15711. https://doi.org/10.1021/jacs.5b10385.
(33) DeGayner, J. A.; Jeon, I.-R.; Sun, L.; Dincă, M.; Harris, T. D. 2D Conductive Iron-Quinoid Magnets Ordering up to Tc = 105 K via Heterogenous Redox Chemistry. *J. Am. Chem. Soc.* **2017**, *139* (11), 4175–4184. https://doi.org/10.1021/jacs.7b00705.
(34) Kitagawa, S.; Kawata, S. Coordination Compounds of 1,4-Dihydroxybenzoquinone and Its Homologues. Structures and Properties. *Coord. Chem. Rev.* **2002**, *224* (1), 11–34. https://doi.org/https://doi.org/10.1016/S0010-8545(01)00369-1.
(35) Lemal, D. M. Perspective on Fluorocarbon Chemistry. *J. Org. Chem.* **2004**, *69* (1), 1–11. https://doi.org/10.1021/jo0302556.
(36) Sini, K.; Bourgeois, D.; Idouhar, M.; Carboni, M.; Meyer, D. Metal–Organic Framework Sorbents for the Removal of Perfluorinated Compounds in an Aqueous Environment. *New J. Chem.* **2018**, *42* (22), 17889–17894. https://doi.org/10.1039/C8NJ03312A.
(37) Herkert, N. J.; Merrill, J.; Peters, C.; Bollinger, D.; Zhang, S.; Hoffman, K.; Ferguson, P. L.; Knappe, D. R. U.; Stapleton, H. M. Assessing the Effectiveness of Point-of-Use Residential Drinking Water Filters for Perfluoroalkyl Substances (PFASs). *Environ. Sci. Technol. Lett.* **2020**, *7* (3), 178–184. https://doi.org/10.1021/acs.estlett.0c00004.
(38) Ehlich Ludovico and Sahalianov, Ihor and Nikic, Marta and Brodský, Jan and Gablech, Imrich and Vu, Xuan Thang and Ingebrandt, Sven and Glowacki, Eric Daniel, J. and M. Direct Measurement of Oxygen Reduction Reactions at Neurostimulation Electrodes. *J. Neural Eng.* **2022**.
(39) de Lourdes Gonzalez-Juarez, M.; Morales, C.; Flege, J. I.; Flores, E.; Martin-Gonzalez, M.; Nandhakumar, I.; Bradshaw, D. Tunable Carrier Type of a Semiconducting 2D Metal–Organic Framework Cu3(HHTP)2. *ACS Appl. Mater. Interfaces* **2022**, *14* (10), 12404–12411. https://doi.org/10.1021/acsami.2c00089.
(40) Duke, A. S.; Dolgopolova, E. A.; Galhenage, R. P.; Ammal, S. C.; Heyden, A.; Smith, M. D.; Chen, D. A.; Shustova, N. B. Active Sites in Copper-Based Metal−Organic Frameworks: Understanding Substrate Dynamics, Redox Processes, and Valence-Band Structure. **2015**. https://doi.org/10.1021/acs.jpcc.5b08053.
(41) Biesinger, M. C. Advanced Analysis of Copper X-Ray Photoelectron Spectra. *Surf. Interface Anal.* **2017**, *49* (13), 1325–1334. https://doi.org/10.1002/SIA.6239.
(42) Ding, S.; Mosher, C.; Lee, X. Y.; Das, S. R.; Cargill, A. A.; Tang, X.; Chen, B.; McLamore, E. S.; Gomes, C.; Hostetter, J. M.; Claussen, J. C. Rapid and Label-Free Detection of Interferon Gamma via an Electrochemical Aptasensor Comprising a Ternary Surface Monolayer on a Gold Interdigitated Electrode Array. *ACS Sensors* **2017**, *2* (2), 210–217. https://doi.org/10.1021/acssensors.6b00581.
(43) Kaushik, A.; Yndart, A.; Kumar, S.; Jayant, R. D.; Vashist, A.; Brown, A. N.; Li, C.-Z.; Nair, M. A Sensitive Electrochemical Immunosensor for Label-Free Detection of Zika-Virus Protein. *Sci. Rep.* **2018**, *8* (1), 9700. https://doi.org/10.1038/s41598-018-28035-3.
(44) Clark, R. B.; Dick, J. E. Electrochemical Sensing of Perfluorooctanesulfonate (PFOS) Using Ambient Oxygen in River Water. *ACS Sensors* **2020**, *5* (11), 3591–3598. https://doi.org/10.1021/acssensors.0c01894.
(45) Barzen-Hanson, K. A.; Roberts, S. C.; Choyke, S.; Oetjen, K.; McAlees, A.; Riddell,

N.; McCrindle, R.; Ferguson, P. L.; Higgins, C. P.; Field, J. A. Discovery of 40 Classes of Per- and Polyfluoroalkyl Substances in Historical Aqueous Film-Forming Foams (AFFFs) and AFFF-Impacted Groundwater. *Environ. Sci. Technol.* **2017**, *51* (4), 2047–2057. https://doi.org/10.1021/acs.est.6b05843.

(46) Voogt, P. de; Sáez, M. Analytical Chemistry of Perfluoroalkylated Substances. *TrAC Trends Anal. Chem.* **2006**, *25* (4), 326–342. https://doi.org/https://doi.org/10.1016/j.trac.2005.10.008.

(47) Ilavsky, J. {\it Nika}: Software for Two-Dimensional Data Reduction. *J. Appl. Crystallogr.* **2012**, *45* (2), 324–328. https://doi.org/10.1107/S0021889812004037.

(48) D. Oosterhout, S.; Savikhin, V.; Zhang, J.; Zhang, Y.; A. Burgers, M.; R. Marder, S.; C. Bazan, G.; F. Toney, M. Mixing Behavior in Small Molecule:Fullerene Organic Photovoltaics. *Chem. Mater.* **2017**, *29* (7), 3062–3069. https://doi.org/10.1021/acs.chemmater.7b00067.